Article

Van der Waals Complexes of Polar Aromatic Molecules: Unexpected Structures for Dimers of Azulene

Manuel Piacenza, and Stefan Grimme

J. Am. Chem. Soc., **2005**, 127 (42), 14841-14848• DOI: 10.1021/ja053613q • Publication Date (Web): 28 September 2005

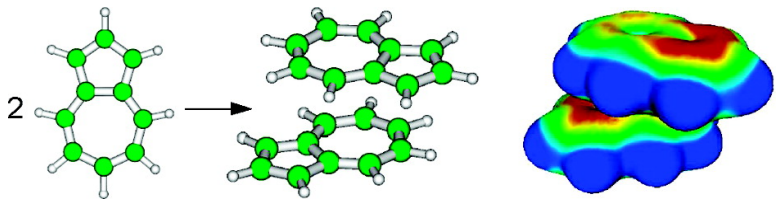

More About This Article

Additional resources and features associated with this article are available within the HTML version:

- Supporting Information
- Links to the 21 articles that cite this article, as of the time of this article download
- Access to high resolution figures
- Links to articles and content related to this article
- Copyright permission to reproduce figures and/or text from this article

View the Full Text HTML

J|A|C|S
ARTICLES
Published on Web 09/28/2005

Van der Waals Complexes of Polar Aromatic Molecules: Unexpected Structures for Dimers of Azulene

Manuel Piacenza and Stefan Grimme*

Contribution from the Theoretische Organische Chemie, Organisch-Chemisches Institut der Universität Münster, Corrensstrasse 40, D-48149 Münster, Germany

Received June 2, 2005; E-mail: grimmes@uni-muenster.de

Abstract: Full geometry optimizations at the dispersion corrected DFT-BLYP/TZV2P level of theory have been performed for dimers of azulene that may serve as a model system for the van der Waals complexes of polar π systems. The structures and binding energies for 11 dimers are investigated in detail. The DFT-D interaction energies have been successfully checked against results from the accurate SCS-MP2/aug-cc-pVTZ approach. Out of the nine investigated stacked complexes, eight have binding energies larger than 7.4 kcal/mol (SCS-MP2) that exceed the value of 7.1 kcal/mol for the best naphthalene dimer. T-shaped arrangements (CH$\cdots\pi$) are significantly less stable. Two out of the three best structures have an antiparallel alignment of the monomer dipole moments in the complex, although the best ones with a parallel orientation are only about 0.5 kcal/mol less strongly bound which points to a minor importance of dipole−dipole interactions to binding. Quite surprisingly, the energetically lowest structure ($\Delta E = -9.2$ kcal/mol) corresponds to a situation where the two seven-membered rings are located almost on top of each other (7−7) and the long molecular axes are rotated against each other by 130°. The 7−7 structural motif is found also in other energetically low-lying structures, and the expected 5−7 (two-side) arrangement is less strongly bound by about 2 kcal/mol. This can be explained by the electrostatic potential of azulene that only partially reflects the charge separation according to the common $4n + 2$ π electron rule. General rules for predicting stable van der Waals complexes of polar π systems are discussed.

1. Introduction

Noncovalent interactions of aromatic complexes that are of great importance in biological systems such as DNA or proteins (see, e.g., ref 1 and refs therein), in material science, or in supramolecular chemistry[2] are mainly determined by a complicated interplay between van der Waals (vdW, also called dispersion) and electrostatic (ES) interactions. Even the adhesive forces that enable geckos to climb walls in either direction are assigned to vdW effects.[3] At shorter intermolecular distances, exchange−repulsion (EXR) contributions, which stem from the Pauli principle, dominate the forces. The ES and EXR contributions can already be described accurately at the Hartree−Fock (HF) level of theory, whereas vdW interactions represent pure electron correlation effects.[4] It is now clear that common Kohn−Sham density functionals which treat electron correlation only in an approximate manner cannot describe vdW interactions (see, e.g., refs 5−9 and refs therein). On the other hand, it is also well established that Møller−Plesset perturbation theory (MP2) which represents the most widely applied ab initio approach for weakly bound complexes tends to overestimate the interaction energies and to underestimate intermolecular distances[10−12] in stacked unsaturated complexes. More sophisticated methods based on coupled-cluster theory[13] (e.g., CCSD(T) or QCISD(T)) are computationally not feasible with reasonably large atomic orbital (AO) basis sets already for medium-sized systems. Recently, one of us further developed an empirical correction scheme for density functional theory calculations (termed DFT-D,[9] see next section) that accounts for vdW interactions by pairwise additive C_6/R^6 potentials. Calculations with this very efficient method have shown promising results for a wide variety of weakly bonded systems[9,14,15] (for related methods, see, e.g., refs 16−18, and for other recent attempts at the DFT/vdW problem, see refs 19−22).

(1) Kannan, N.; Vishveshwara, S. *Protein Eng.* **2000**, *13*, 753.
(2) Bhattacharyya, R.; Samanta, U.; Chakrabarti, P. *Protein Eng.* **2002**, *15*, 91. Meyer, E. A.; Castellano, R. K.; Diederich, F. *Angew. Chem., Int. Ed.* **2003**, *42*, 1210.
(3) Autumn, K.; Sitti, M.; Liang, Y. A.; Peattie, A. M.; Hansen, W. R.; Sponberg, S.; Kenny, T. W.; Fearing, R.; Israelachvili, J. N.; Full, R. J. *Proc. Natl. Acad. Sci. U.S.A.* **2002**, *99*, 12252.
(4) Stone, A. J. *The Theory of Intermolecular Forces*; Oxford University Press: Oxford, NY, 1997.
(5) Kristyan, S.; Pulay, P. *Chem. Phys. Lett.* **1994**, *229*, 175.
(6) Hobza, P.; Sponer, J.; Reschel, T. *J. Comput. Chem.* **1995**, *11*, 1315.
(7) Rappé, A. K.; Bernstein, E. R. *J. Phys. Chem. A* **2000**, *104*, 6117.
(8) Allen, M.; Tozer, D. J. *J. Chem. Phys.* **2002**, *117*, 11113.
(9) Grimme, S. *J. Comput. Chem.* **2004**, *25*, 1463.
(10) Hobza, P.; Selzle, H. L.; Schlag, E. W. *J. Phys. Chem.* **1996**, *100*, 18790.
(11) Sinnokrot, M. O.; Valeev, W. F.; Sherrill, C. D. *J. Am. Chem. Soc.* **2002**, *124*, 10887.
(12) Tsuzuki, S.; Honda, K.; Uchimaru, T.; Mikami, M. *J. Chem. Phys.* **2004**, *120*, 647.
(13) Helgaker, T.; Jørgensen, P.; Olsen, J. *Molecular Electronic-Structure Theory*; J. Wiley: New York, 2000.
(14) Zou, B.; Dreger, K.; Mück-Lichtenfeld, C.; Grimme, S.; Schäfer, H. J.; Fuchs, H.; Chi, L. *Langmuir* **2005**, *21*, 1364.
(15) Piacenza, M.; Grimme, S. *Chem. Phys. Chem.* **2005**, *6*, 1554.
(16) Wu, X.; Vargas, M. C.; Nayak, S.; Lotrich, V.; Scoles, G. *J. Chem. Phys.* **2001**, *115*, 8748.
(17) Wu, Q.; Yang, W. *J. Chem. Phys.* **2002**, *116*, 515.
(18) Elstner, M.; Hobza, P.; Frauenheim, T.; Suhai, S.; Kaxiras, E. *J. Chem. Phys.* **2001**, *114*, 5149.

Scheme 1

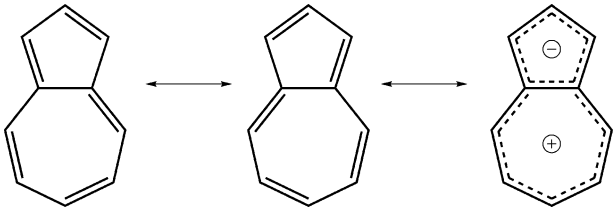

A well-examined example for aromatic vdW complexes is the benzene dimer. According to recent high-level ab initio calculations,[11,23−26] the so-called T-shaped and parallel displaced structures are found to be the lowest in energy (interaction energies of about −2.5 to −3.0 kcal/mol[24,25,27]) and their energetic difference is below 0.1 kcal/mol. However, the benzene monomer possesses no dipole moment, and thus, mainly quadrupole interactions contribute to the ES forces. This also holds true for stacked naphthalene dimers[12] that are approximately 2 times more strongly bound (for the empirical treatment of larger clusters of aromatic molecules, see ref 28). Note that the terms "π stacked" or "$\pi-\pi$ stacking" should merely be used as geometrical (structural) descriptors but that specific (distinguished) attractive interactions between π electrons in such systems do not exist.[29]

Azulene ($C_{10}H_8$) is an isomer of naphthalene, but with significantly different properties. Similar to naphthalene, it is a planar hydrocarbon possessing 10 π electrons, but aside from two electronically neutral resonance structures, there is the possibility of a zwitterionic form, with a negatively charged five-membered and a positively charged seven-membered ring that both formally obey Hückel's $4n + 2$ rule (see Scheme 1). The charge separation of the zwitterionic form is considered as the reason for the relatively large dipole moment of $\mu = 0.8-1.08$ D[30−32] (1 D = 3.36×10^{-30} cm). Furthermore, as a nonalternant hydrocarbon, azulene has more unusual properties (e.g., its blue color or relatively high polarizability[33]) that are exploited in, e.g., advanced polymers, optical materials, or liquid crystals (see ref 34 and refs therein). In this study, we want to investigate the influence of the polar character of the azulene monomer upon formation of dimer complexes. This continues previous theoretical studies on this specific compound[35] and on polar aromatic vdW complexes in general.[15] Intuitively, one would expect that in optimal dimer arrangements the (at least in part) negatively charged five-membered ring of one monomer would sit on top of the positively charged seven-membered ring of the other fragment (denoted as a 5−7 arrangement in the following). As will be shown here, this obvious structure is relatively high in energy and many other quite unexpected orientations are much better bound. Note that, because of the complexity of the dimer potential energy surface, only full geometry optimizations as performed here can provide conclusive answers. More detailed insights into the complicated interplay among ES, EXR, and vdW contributions may lead to a better understanding of the structures of polar aromatic complexes with low symmetry, in general, that are very common in nature and supramolecular applications. In this sense, the azulene dimer may serve as a model system with structural and electronic motifs that appear also in fullerenes and carbon nanotubes.

2. Computational Details and Validation of Methods

As already mentioned in the Introduction, the DFT-D approach[9] makes use of a pairwise additive C_6/R^6 type potential to account for long-range dispersion effects that are notoriously poor (or even nonexistent) with current density functionals (for details, see ref 9). In this approach, the dispersion correction that is added to the usual DFT energy is given as

$$E_{\mathrm{disp}} = -s_6 \sum_{i=1}^{N_{\mathrm{at}}-1} \sum_{j=i+1}^{N_{\mathrm{at}}} \frac{C_6^{ij}}{R_{ij}^6} f_{\mathrm{damp}}(R_{ij})$$

where N_{at} is the number of atoms in the system, C_6^{ij} is the dispersion coefficient for atom pair ij, s_6 is a functional-specific scaling factor, and R_{ij} is the interatomic distance. To avoid near singularities for small distances, a damping function of the type

$$f_{\mathrm{damp}}(R_{ij}) = \frac{1}{1 + \mathrm{e}^{-\alpha(R^{ij}/R_0^{ij}-1)}}$$

is used where R_0 is the sum of atomic van der Waals radii and $\alpha = 23$. The C_6^{ij} coefficients are calculated as an average of atomic C_6 parameters as

$$C_6^{ij} = 2\frac{C_6^i C_6^j}{C_6^i + C_6^j}$$

For carbon and hydrogen, C_6 coefficients of 1.65 and 0.16 J nm^6 mol^{-1} and van der Waals radii of 161 and 111 pm, respectively, are used.[9] The s_6 parameter has been optimized for various pure density functionals.[9] In this work, we tested the well-established BLYP functional[36,37] and the recently introduced meta-GGA functional TPSS.[38] The corresponding s_6 factors are 1.4 (BLYP) and 1.1 (TPSS). Because the calculated binding energies for the two density fuctionals showed at most a 0.3 kcal/mol difference (and furthermore, both gave almost identical complex geometries), we decided to neglect the TPSS results and all DFT-D data thus refer to the BLYP functional.

All calculations were performed on a parallel LINUX-PC-cluster using the TURBOMOLE 5.6[39,40] program suite. The *resolution of*

(19) Andersson, Y.; Langreth, D. C.; Lundqvist, B. I. *Phys. Rev. Lett.* **1996**, *76*, 102.
(20) von Lilienfeld, O. A.; Tavernelli, I.; Röthlisberger, U.; Sebastiani, D. *Phys. Rev. Lett.* **2004**, *93*, 153004.
(21) Becke, A. D.; Johnson, E. R. *J. Chem. Phys.* **2005**, *122*, 154104.
(22) Furche, F.; Voorhis, T. V. *J. Chem. Phys.* **2005**, *122*, 164106.
(23) Grimme, S. *J. Chem. Phys.* **2003**, *118*, 9095.
(24) Sinnokrot, M. O.; Sherrill, C. D. *J. Phys. Chem. A* **2004**, *108*, 10200.
(25) Hesselmann, A.; Jansen, G.; Schütz, M. *J. Chem. Phys.* **2005**, *122*, 014103.
(26) Zhao, Y.; Truhlar, D. G. *J. Phys. Chem. A* **2005**, *109*, 4209.
(27) Tsuzuki, S.; Honda, K.; Uchimura, T.; Mikami, M.; Tanabe, K. *J. Am. Chem. Soc.* **2002**, *124*, 104.
(28) Rapacioli, M.; Calvo, F.; Spiegelman, F.; Joblin, C.; Wales, D. J. *J. Phys. Chem. A* **2005**, *109*, 2487.
(29) The intermolecular C_6 coefficients of unsaturated systems compared to those of saturated systems are larger by about 10−20% for, e.g., hydrocarbons mainly because of the lower excitation energies of the former. This, however, does not justify the use of the term $\pi-\pi$ interactions, in a sense that π electrons are specifically interacting (binding) with (to) each other.
(30) Nelson, R. D., Jr.; Lide, D. R., Jr.; Maryott, A. A. *1967 Selected Values of electric dipole moments for molecules in the gas phase*; National Standard Reference Data Series, NSRDS-NBS10. http://www.nist.gov/srd/nsrds.htm).
(31) Tobler, H. J.; Bauder, A.; Günthard, H. H. *J. Mol. Spectrosc.* **1965**, *18*, 239.
(32) Anderson, A. G.; Steckler, B. M. *J. Am. Chem. Soc.* **1959**, *81*, 4941.
(33) The static dipole polarizabilities at the BLYP/TZV2P level are 118.3 and 128.2 a_0^3 for naphthalene and azulene, respectively.
(34) Robinson, R. E.; Holovics, T. C.; Deplazes, S. F.; Powell, D. R.; Lushington, G. H.; Thompson, W. H.; Barybin, M. V. *Organometallics* **2005**, *24*, 2386.
(35) Grimme, S. *Chem. Phys. Lett.* **1993**, *201*, 67.
(36) Becke, A. D. *Phys. Rev. A* **1988**, *38*, 3098.
(37) Lee, C.; Yang, W.; Parr, R. G. *Phys. Rev. B* **1988**, *37*, 785.
(38) Tao, J.; Perdew, J. P.; Staroverov, V. N.; Scuseria, G. E. *Phys. Rev. Lett.* **2003**, *91*, 146401.
(39) R. Ahlrichs et al. *TURBOMOLE*, version 5.6; Universität Karlsruhe: 2003. See also: http://www.turbomole.com.

identity (RI) approximation[41,42] was employed in all DFT, MP2, and QCISD(T) calculations, and the corresponding auxiliary basis sets were taken from the TURBOMOLE basis set library.[43] All structures have been fully optimized at the DFT-D level without any symmetry constraints (resulting higher symmetries are reported, however) using an AO basis set of valence triple-ζ quality with two sets of polarization functions (2d2p, denoted as TZV2P).[44] The optimizations have been started from various (unsymmetrical) initial dimer arrangements so that we can be quite sure to present the true lowest minima on the potential energy surface (PES). Note that some of the structures may not be true minima on the PES because of the symmetry restrictions applied. This is, however, not of practical relevance as these structures mostly have model character, and the PES are very flat around these stationary points. For the most stable structure (**7**), we also calculated the (harmonic) vibrational frequencies. The structure is characterized as a true minimum, and the zero-point vibrational energy (ZPVE) correction to the binding energy amounts to 0.7 kcal/mol.

Subsequent single-point calculations were carried out with Dunning's correlation-consistent augmented polarized triple-ζ basis set (aug-cc-pVTZ[45,46]). The SCS-MP2 model[23] represents a recently introduced improved version of the standard Møller−Plesset perturbation theory, in which the correlation energy is partitioned into parallel- and antiparallel-spin components that are separately scaled. It provides significantly improved energetics compared to those of standard MP2 for a wide variety of chemical systems, often reaching QCISD(T) accuracy, and also corrects for the systematic overestimation of MP2 for vdW interactions in unsaturated systems.[23,47,48] All MP2 and SCS-MP2 interaction energies (ΔE) have been corrected for basis set superposition error (BSSE) following the counterpoise (CP) method.[49] The small BSSE effects in the case of DFT-D which are typically <5% of ΔE have been absorbed into the empirical potential.[9]

To evaluate the quality of the SCS-MP2 and DFT-D methods for our problem, we perform additional QCISD(T)[50] calculations for a typical structure. The dimer **1** with C_{2h} symmetry (see Figure 1) is used. Because QCISD(T) calculations are computationally demanding, they are limited to the aug-cc-pVDZ basis set and are not corrected for BSSE. It is, however, well-known that the basis set dependence is very similar for MP2 and QCI/CC calculations such that the QCISD(T)/aug-cc-pVDZ values together with SCS-MP2 basis set increments can be taken as the most reliable reference values. The results are listed in Table 1.

The CP corrected MP2 and SCS-MP2 interaction energies ΔE are approximately 1 kcal/mol lower for the triple-ζ basis set compared with those from the double-ζ basis set. The uncorrected QCISD(T) and SCS-MP2 values differ by only 1.3 kcal/mol (about 10% of ΔE), whereas MP2 is too low by 5.4 kcal/mol and QCISD is too high by 3 kcal/mol (a similar behavior is found for benzene and pyridine dimers[11,15,24]). Moreover, it was shown[15] that the BSSE contribution with the aug-cc-pVDZ basis set is about 50% for both SCS-MP2 and QCISD(T) methods. From these results, it is clear that SCS-MP2 represents a very accurate method for structures of this type and that standard MP2 should be avoided for stacked aromatics. Note further that the SCS-MP2/aug-cc-pVTZ interaction energy calculated for the naphthalene dimer (−7.1 kcal/mol, see section 3.1) agrees to about 1 kcal/mol with the estimated CCSD(T) values from ref 12. Taking the complete basis-set-extrapolated SCS-MP2 result (about −9 kcal/mol) and correcting for the difference with respect to QCISD(T) at the aug-cc-pVDZ level (10%) lead finally to an estimated ΔE of about -8 ± 0.3 kcal/mol. Compared to this reference value, the DFT-D method yields binding energies that are slightly too weak (by about 2 kcal/mol) but can still be considered as quite accurate (at least when compared to, e.g., standard MP2). The reason for this slight underbinding of DFT-D for the azulene dimer compared to that of other stacked aromatic complexes may be the special electronic character of azulene that leads to a higher polarizability and thus larger dispersion interactions that cannot be described completely by the (molecule-independent) C_6 coefficients in DFT-D.

Table 1. Binding Energies (ΔE) of the C_{2h} Symmetric Azulene Dimer (**1**) with Different Methods and AO Basis Sets[a]

	−ΔE (kcal/mol)			
method	aug-cc-pVDZ		aug-cc-pVTZ	
MP2	11.8	(19.0)	12.7	(15.8)
SCS-MP2	7.7	(14.9)	8.5	(11.7)
QCISD		(10.6)		
QCISD(T)		(13.6)		
DFT-D	5.0	(6.3)	5.6	(5.9)

[a] The molecular geometry has been optimized at the DFT-D-BLYP/TZV2P level of theory. CP uncorrected values are given in parentheses.

Table 2. Intermolecular Distances (R in Å) and Binding Energies (ΔE in kcal/mol) of Azulene Dimers[a]

				−ΔE		
dimer	type[b]	symmetry	R	DFT-D[c]	MP2[d]	SCS-MP2[e]
7	SR	C_2	3.43	7.2	14.4 (17.8)	9.2 (13.2)
3	SA	C_1	3.43	6.1	3.0 (16.1)	8.7 (12.1)
1	SA	C_{2h}	3.46	5.9	2.7 (15.8)	8.5 (11.7)
6	SP	C_1	3.42	5.7	2.6 (15.7)	8.3 (11.6)
5	SP	C_s	3.47	5.2	11.9 (14.9)	7.7 (10.9)
9	SR	C_2	3.54	5.2	11.8 (14.9)	7.8 (11.0)
8	SR	C_1	3.44	5.2	11.4 (14.3)	7.5 (10.6)
2	SA	C_{2h}	3.49	4.9	1.5 (14.5)	7.4 (10.5)
10	T	C_s	2.58[e]/2.63[f]	4.1	6.5 (9.2)	4.5 (7.4)
11	T	C_s	2.64[e]/2.53[f]	4.0	7.4 (8.7)	5.5 (6.9)
4	SP	C_{2v}	3.79	3.2	8.8 (11.4)	5.6 (8.3)
12[g]		C_i	3.45	5.6	10.8 (13.8)	7.1 (10.2)

[a] For MP2 and SCS-MP2, BSSE uncorrected values are given in parentheses. [b] SR: stacked rotated. SA: stacked antiparallel. SP: stacked parallel. T: CH···π. [c] TZV2P AO basis set. [d] aug-cc-pVTZ AO basis set. [e] Distance of the hydrogen atom to the five-membered ring center. [f] Distance of the hydrogen atom to the seven-membered ring center. [g] Naphthalene dimer.

A quite difficult task is the proper geometrical description of the intermolecular distances (denoted as R in Table 2) in such low-symmetry complexes. We decided to describe the stacked complexes by their interplanar distances. In the case of slightly tilted dimers (i.e., **3**, **6**, and **7**), we took the average of the closest and farthest distances. In the T-shaped dimers, R refers to the distance between a hydrogen atom and the centers of the five- or seven-membered rings.

To put our discussion on the origin of binding on a more profound basis, we performed energy decomposition analyses (EDA) at the DFT-D-BLYP/TZV2P level of theory to distinguish the various contributions to the total binding energy. The EDA has proven to give detailed information about the nature of chemical bonding[51−53] as well as,

(40) Ahlrichs, R.; Bär, M.; Häser, M.; Horn, H.; Kölmel, C. *Chem. Phys. Lett.* **1989**, *162*, 165.
(41) Eichkorn, K.; Treutler, O.; Öhm, H.; Häser, M.; Ahlrichs, R. *Chem. Phys. Lett.* **1995**, *240*, 283.
(42) Weigend, F.; Häser, M.; Ahlrichs, R. *Theor. Chem. Acc.* **1997**, *97*, 331.
(43) The basis sets are available from the TURBOMOLE homepage via the FTP Server Button (in the subdirectories basen, jbasen, and cbasen). See http://www.turbomole.com.
(44) Schäfer, A.; Huber, C.; Ahlrichs, R. *J. Chem. Phys.* **1994**, *100*, 5829.
(45) Dunning, T. H. *J. Chem. Phys.* **1989**, *90*, 1007.
(46) Kendall, R. A.; Dunning, T. H.; Harrison, R. J. *J. Chem. Phys.* **1992**, *96*, 6796.
(47) Gerenkamp, M.; Grimme, S. *Chem. Phys. Lett.* **2004**, *392*, 229.
(48) Grimme, S. *Chem.−Eur. J.* **2004**, *10*, 3423.
(49) Boys, S. F.; Bernardi, F. *Mol. Phys.* **1970**, *19*, 553.
(50) Raghavachari, K.; Trucks, G. W.; Pople, J. A.; Head-Gordon, M. *Chem. Phys. Lett.* **1989**, *157*, 479.
(51) Morokuma, K. *J. Chem. Phys.* **1971**, *55*, 1237.
(52) Kitaura, K.; Morokuma, K. *Int. J. Quantum Chem.* **1976**, *10*, 325.
(53) Bickelhaupt, F. M.; Baerends, E. J. Kohn−Sham Density Functional Theory: Predicting and Understanding Chemistry. In *Reviews in Computational Chemistry*; Lipkowitz, K. B., Boyd, D. B., Eds.; Wiley-VCH: New York, 2000; Vol. 15.

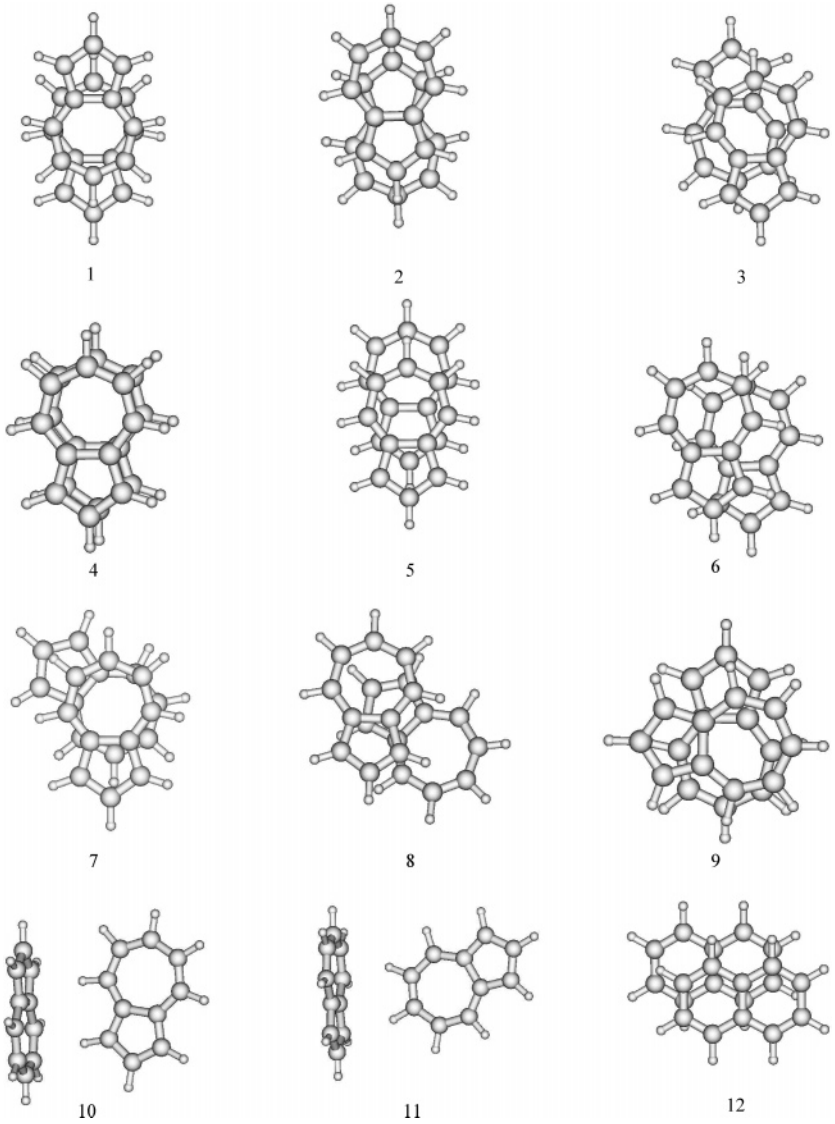

Figure 1. Optimized DFT-D-BLYP/TZV2P structures of the investigated azulene (**1**−**11**) and naphthalene (**12**) dimers.

recently, for the interactions in DNA base pairs.[54] The method has been discussed in detail before and is only briefly described here. The formation of bonding between two fragments is divided into three physically plausible steps. In the first step, the fragment electronic densities (in the frozen geometry of the supermolecule) are superimposed which yields the quasiclassical electrostatic interaction energy ΔE_{ES}. Antisymmetrizing of the product of monomer wave functions yields a repulsive energy term that is usually called Pauli (exchange) repulsion (ΔE_{EXR}). In the final step, the molecular orbitals are allowed to relax to their final form which yields the (usually stabilizing) polarization, orbital, and charge-transfer interaction energy ΔE_{POCT}. The sum $\Delta E = \Delta E_{ES} + \Delta E_{EXR} + \Delta E_{POCT} + \Delta E_{disp}$, which also includes the dispersion energy term from the DFT-D approach, differs from the true interaction energy by the energy necessary to bring the optimum monomer geometries into the form they have in the supermolecule (ΔE_{def}). ΔE_{def} is almost negligible ($\leq$0.1 kcal/mol) in all our cases and is not discussed further. The EDA results for some aromatic vdW complexes at the DFT-D-BLYP level have been compared to those from a more sophisticated symmetry-adapted perturbation theory (SAPT) analysis[25,55] of the interaction energies from which very similar corresponding values and qualitative pictures emerged.

(54) Swart, M.; Fonseca, C.; Bickelhaupt, F. M. *J. Am. Chem. Soc.* **2004**, *126*, 16718.
(55) Sinnokrot, M. O.; Sherrill, C. D. *J. Am. Chem. Soc.* **2003**, *126*, 7690.

3. Results

3.1. Structures and Energies. In our study, we included 11 dimer structures of azulene, consisting of nine stacked (**1**−**9**, denoted as S) and two CH···π (**10**, **11**, T-shaped, denoted as T) complexes that are shown in Figure 1. The first three structures (**1**−**3**) correspond to stacked complexes with an antiparallel orientation with respect to the monomer dipole moments (termed SA), and **4**−**6** have the reverse (parallel) orientation (SP). In the stacked complexes **7**−**9**, the monomers are rotated against each other (SR). As an apolar reference structure, we chose the C_i symmetric naphthalene dimer (**12**) that corresponds to a displaced arrangement similar to that of graphite. The results of the DFT-D, MP2, and SCS-MP2 calculations are gathered in Table 2 and are shown graphically in Figure 2.

All 11 dimer structures are relatively strongly bound, and their DFT-D interaction energies are found in a range from −3.2 to −7.2 kcal/mol. Note that these structures are not bound at all at the pure DFT level with (positive) interaction energies between 1−2 (T) and about 6 kcal/mol (S). What comes as a bit of a surprise is the fact that the C_2 symmetric rotated complex

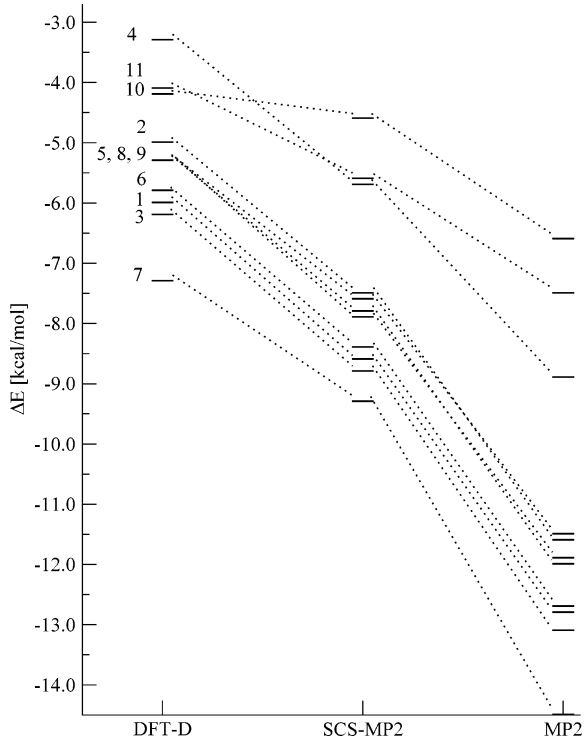

Figure 2. Energetic ordering of azulene dimers with DFT-D, SCS-MP2, and MP2 methods.

(**7**) is the most stable structure rather than one of the antiparallel structures (**1**−**3**). Energetically slightly higher lying are the three stacked complexes **3**, **1**, and **6**, with interaction energies of −6.1, −5.9, and −5.7 kcal/mol, respectively. Interestingly, in **1**, the displacement along the long axis of the molecule is such that both seven-membered rings are almost on top of each other (7−7 orientation). Structures **3** and **6** correspond to short-axis displaced SA and SP dimers, respectively, which are energetically and structurally similar to the C_i symmetric naphthalene dimer **12** ($\Delta E = -5.6$ kcal/mol). Note that **3** and **6** are *both* more strongly bound than **12** and that the difference between the SA and SP orientation amounts to only 0.4 kcal/mol. These observations already indicate a minor importance of the monomer dipole moment to binding. The next group consists of structures **5**, **8**, and **9** with DFT-D interaction energies of about −5.2 kcal/mol. Again, quite surprisingly, the SA structure **2** with two 5−7 alignments of the rings (that is intuitively expected to be favored) is relatively high in energy (−4.9 kcal/mol). With binding energies of −4.1 and −4.0 kcal/mol, the two T-shaped dimers (**10** and **11**) are about 1 kcal/mol less stable than the weakest bound stacked complexes. Least stable is the face-to-face structure **4** (−3.2 kcal/mol) which corresponds to the D_{6h} form of the benzene dimer that is also higher in energy than its corresponding T-shaped or displaced structures. Regarding the interplanar distances *R*, most stacked structures are found in a typical range of 3.4−3.5 Å. Structure **4** shows a rather large value of 3.79 Å, which is in agreement with its low binding energy.

Comparing the DFT-D and CP corrected SCS-MP2 and MP2 values, we can conclude that conventional MP2 clearly overestimates binding. The CP corrected MP2 values for the stacked dimers (**1**−**9**) are approximately 6−7 kcal/mol more negative than the DFT-D values. For the T-shaped forms, this difference is reduced to 2.4 (**10**) and 3.4 kcal/mol (**11**). All stacked systems show a BSSE of about 20% of the interaction energy. For the T-shaped complex **10**, it is 30%, and for **11**, it is only 15%. This deviation can be explained by the different orientations of the fragments, as the average intermolecular distances are smaller for **10**. The SCS-MP2 binding energies are somewhat higher than the DFT-D values but are significantly smaller compared to those of standard MP2. The differences between MP2 and SCS-MP2 are about 4 kcal/mol for stacked structures and about 2 kcal/mol for T-shaped structures. Compared to that of DFT-D, this difference is only about 1.5−2.5 kcal/mol, and it is again significantly lower for the T-shaped structures (**10** = 0.4 kcal/mol, **11** = 1.4 kcal/mol). Nevertheless, the qualitative picture of the relative stabilities stays more or less identical, as can be seen in Figure 2. The ordering of and within the previously discussed groups is maintained with DFT-D. The only differences are found for the T-shaped structures (**10** and **11**) and the dimer **4**. Complex **10** is destabilized compared to **11** in both the scaled and unscaled MP2 calculations. The difference is approximately 1 kcal/mol. As mentioned above, the stabilization of T-shaped structures when going from DFT-D to MP2 is smaller than for the stacked complexes. This leads to a change in the order of stability, and **4** becomes more stable than **10** and **11** in the ab initio calculations.

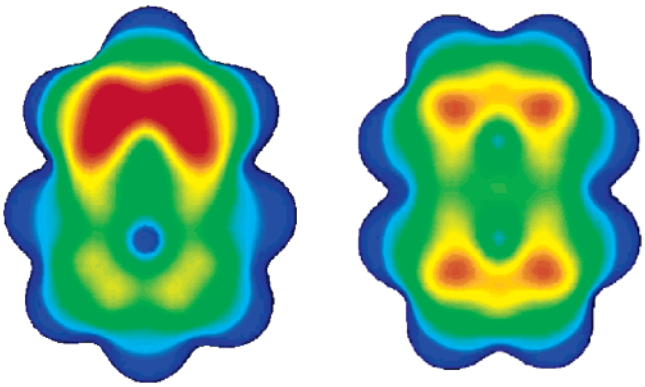

Figure 3. Plot of the electrostatic potential (ESP) for the azulene (left) and naphthalene (right) molecules (BLYP/TZV2P) on the isodensity surface defined by a value of 0.005 a_0^{-3}. The color-coded potential (when interacting with a positive unit charge) ranges from −13 (red) to 13 (blue) kcal/mol. The zero of the ESP is given by the green/blue border.

In summary, we find, for the most stable azulene dimers, arrangements with rotated or unusually shifted monomers that are at first sight quite unexpected. These findings suggest a minor importance of the permanent dipole moment for the relative orientation of the monomers in the dimer. Furthermore, quite surprisingly, in the three best complexes, the (formally) positively charged seven-membered rings are stacked quite closely on top of each other (7−7 alignment). This prompts us to question the role of the electrostatic interactions in these structures, which is investigated in more detail below.

3.2. Analysis of the Interactions. Before continuing with an analysis of the various contributions to the intermolecular binding, the structural results presented above suggest a closer look at the electrostatic potential (ESP) of the azulene molecule (see Figure 3 and for previous use of ESPs in the prediction of weak binding, see, e.g., ref 56). Although the polar character of azulene is clearly visible from the ESP (especially when

(56) Gadre, S. R.; Deshmukh, M. M.; Chakraborty, T. *Chem. Phys. Lett.* **2004**, *384*, 350.

Table 3. Energy Decomposition Analysis (in kcal/mol) for Azulene Dimers at the DFT-D-BLYP/TZV2P Level of Theory.

dimer	type[a]	ΔE_{EXR}	ΔE_{ES}	ΔE_{POCT}	ΔE_{disp}	ΔE
7	SR	14.9	−5.0	−4.2	−13.1	−7.3
3	SA	12.4	−3.9	−2.7	−12.0	−6.2
1	SA	12.0	−3.6	−2.6	−11.8	−6.0
6	SP	12.3	−3.6	−2.6	−11.8	−5.8
5	SP	11.7	−2.9	−2.3	−11.7	−5.3
9	SR	10.5	−2.6	−1.7	−11.6	−5.3
8	SR	11.0	−3.2	−2.3	-10.9	−5.4
2	SA	11.1	−2.6	−2.0	−11.5	−5.0
10	T	6.0	−2.6	−1.8	−5.9	−4.2
11	T	5.9	−2.6	−1.6	−5.7	−4.0
4	SP	7.0	−0.5	−0.8	−9.0	−3.3
12[b]		11.5	−3.3	−2.2	−11.6	−5.7

[a] SR: stacked rotated. SA: stacked antiparallel. SP: stacked parallel. T: CH···π. [b] Naphthalene dimer.

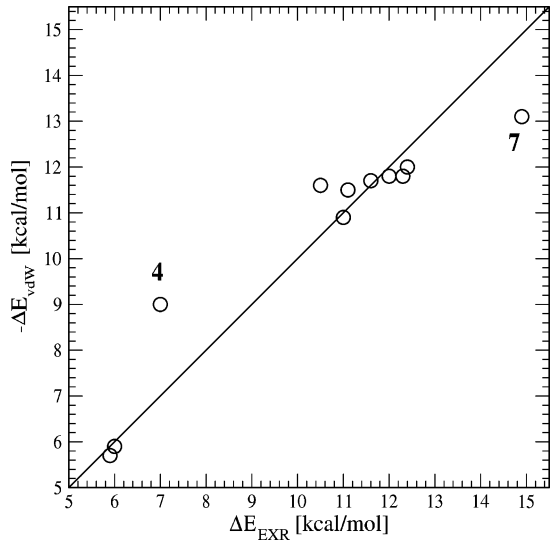

Figure 4. Exchange repulsion vs vdW contributions to binding (DFT-D-BLYP/TZV2P) for the investigated azulene complexes. The solid line starts at the origin and has a slope of unity.

compared with that of the isomer naphthalene), it also turns out that the Hückel picture with negatively charged five-membered rings and positively charged seven-membered rings represents a gross overestimate. Regions of strong negative potential (corresponding to regions of accumulated negative charge) are only found close to C1/C3, and the region of the seven-membered ring shows a slight negative potential (in green) that is close to zero. This already explains, at least in part, why these rings tend to come quite close together, thereby minimizing electrostatic repulsion. According to this picture, the positive charge at the hydrogens H4−H8 together with the negative charge at C1/C3 is mainly responsible for the permanent dipole moment of azulene.

To get an even deeper insight into the competing energy contributions, we decided to perform an energy decomposition analysis (EDA) at the DFT-D BLYP/TZV2P level of theory. The results are gathered in Table 3. The main (absolute) contributions of about 10−15 kcal/mol to the total interaction energies stem from the exchange−repulsion (ΔE_{EXR}) and from the dispersion term (ΔE_{disp}). Noticeably, both contributions are of similar size for most structures (but of different sign) and thus compensate almost quantitatively, as depicted in Figure 4. Interestingly, a relation of the form $\Delta E_{EXR} \approx -\Delta E_{disp}$ has also been noticed in the SAPT analysis of benzene complexes.[25,55] It thus seems to be a general characteristic of aromatic vdW complexes, although, certainly, more investigations are necessary to clarify this point. Significant deviations from this relation are only found for the most strongly and most weakly bound complexes **7** and **4**. In the latter dimer, this can be explained mainly by the relatively large intermolecular distance (and the different R dependencies for ΔE_{EXR} and ΔE_{disp}, respectively).

The remaining contributions, i.e., E_{ES} and E_{POCT}, are always attractive in our cases. Considering only the stacked complexes, these values appear rather uniform ($-\Delta E_{ES} = 2.5-3.9$ kcal/mol, $-\Delta E_{POCT} = 2.0-2.7$ kcal/mol). The exceptions are again the most stable (**7**) and the most unstable dimer (**4**), where much larger and smaller ΔE_{ES} and ΔE_{POCT} values are calculated. The two best SA structures (**1** and **3**) are stabilized by slightly more attractive ES and POCT components than the analogous SP arrangements (**5** and **6**). Note, however, that, quite unexpectedly, this does not hold true for the SA structure **2** with the two 5−7 interactions. The most stable structure **7** not only has stronger attractive contributions than the other complexes but also the ΔE_{EXR} term is 1.8 kcal/mol larger compared to that of ΔE_{disp}. This, however, is overcompensated by the ES and, in particular, POCT parts that are both much lower (by 20−30%) compared to all other complexes. Note further that, compared to the unpolar reference system naphthalene, the stacked azulene dimers **1**, **3**, **6**, and **7** that are more strongly bound also have lower ΔE_{ES} and ΔE_{POCT} values, whereas the reverse is true for **2**, **5**, **8**, and **9** that have lower absolute ΔE values than **12**.

Finally, we want to consider again the question of the contribution of the dipole moment to binding and also show how the distinct energy contributions depend on the intermolecular distances. This is of particular importance because the fully optimized structures have different R values, and the data in Table 3 thus provide only a limited amount of information. As an example, we use two idealized structures of **1** and **4** with perfectly coplanar monomers and varied only the intermolecular distance. The dimers **1** and **4** were chosen because they represent similar structures, but with an opposite relative orientation of the monomer dipole moments. The resulting potential energy curves are displayed in Figure 5.

As discussed above, it is clearly seen that the two major contributions to the total binding energies stem from the EXR and vdW terms. The vdW curves are very similar for both systems, and the values for **4** are found just slightly below the corresponding values for **1**. This (small) difference can be explained by the larger average interatomic distances in **1** that have their origin in the displaced character of the complex, whereas in **4**, the atoms are exactly on top of each other. For the EXR term, the differences are opposite and larger. At 3.4 Å, the EXR contribution disfavors **4** by 3.2 kcal/mol, and at 3.9 Å, it is still 0.7 kcal/mol. Somewhat unexpectedly, the electrostatic contributions are very similar for both structures and thus cannot explain the very different stabilities of the two complexes. For smaller distances, the ES terms are almost identical and the differences increase only slightly (to about 0.5 kcal/mol) at larger R's. This again points to a minor role of the dipole−dipole interactions in binding and agrees with the analysis of the spatial form of the ESP for the azulene monomer (see Figure 3). The behavior of the remaining ΔE_{POCT} contributions is also interesting. At 3.4 Å, these values differ significantly by 1.3 kcal/mol in favor of the SA form, and at 3.9 Å, this

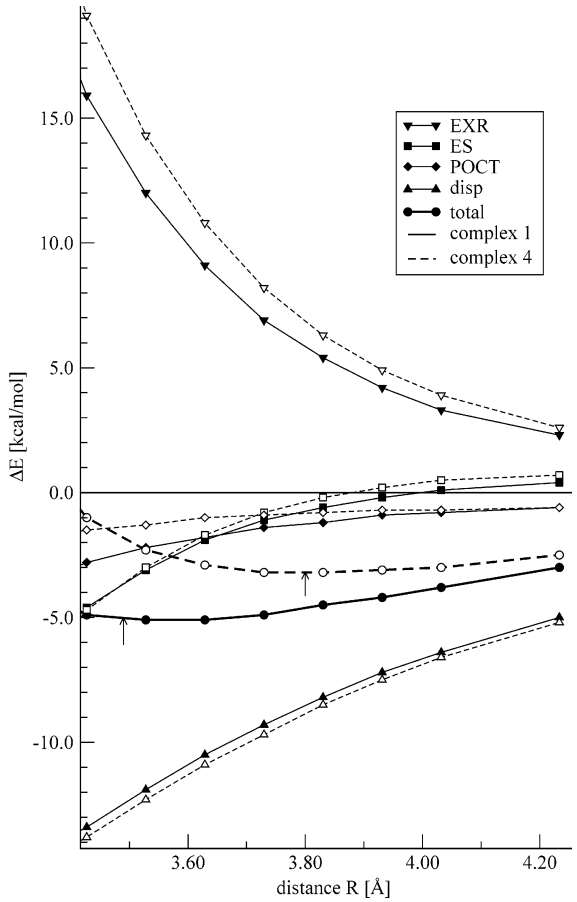

Figure 5. Contributions to the DFT-D-BLYP/TZV2P binding energies of azulene dimers **1** (solid line) and **4** (dashed line) at various intermolecular distances. The arrows mark the minima in the optimized structures, which differ from the minima of the curves because of the use of unrelaxed monomer geometries.

difference is still 0.4 kcal/mol. This can be explained by a partial overlap of seven- with five-membered ring wave function parts in the antiparallel aligned complex **1** that allow easier polarization or charge transfer than in **4**. Thus, in summary, this analysis emphasizes that the POCT effects are more important for the relative energies than the static interactions of the charge distributions. This view is supported by the results of an EDA performed for all stacked structures with a fixed interplanar distance of 3.5 Å (data not shown). In this model, the energetic ordering of the dimers is most strongly related (with a linear correlation coefficient of $r = 0.86$) to the ΔE_{POCT} term.

4. Conclusions

Using full geometry optimizations at the dispersion corrected DFT-BLYP level of theory, we calculated the structures and binding energies for 11 dimers of azulene. The results have been compared to those obtained for the most stable dimer of the valence isomer naphthalene. The DFT-D interaction energies have been successfully checked against results from the SCS-MP2/aug-cc-pVTZ approach that performs similarly to "state-of-the-art" coupled-cluster methods. The diversity of the dimer structures found and the flatness of the corresponding potential energy hypersurface may explain the experimentally observed disordered crystal structure.[57] Out of the nine investigated stacked complexes, eight have binding energies higher than 7.4 kcal/mol (SCS-MP2) that exceed the value of 7.1 kcal/mol for the best naphthalene dimer structure. T-shaped arrangements with CH$\cdots\pi$ contacts are significantly less stable. Two out of the three best structures have an antiparallel alignment of the monomer dipole moments in the complex (SA), although the best SP structures (parallel orientation) are only about 0.5 kcal/mol less strongly bound. This and the results of an energy decomposition analysis (EDA) of the binding energies for all dimers and for two structures at several intermolecular distances point to a minor importance of dipole−dipole interactions to binding in azulene dimers. At first sight, quite surprisingly, the energetically lowest structure corresponds to a situation where the seven-membered rings are located almost on top of each other (7−7) and the long molecular axes are rotated against each other by 130°. The 7−7 structural motif is found also in two other energetically favored structures, and the 5−7 arrangements (i.e., structures **2** and **5** that are expected on the basis of Hückel theory) are less strongly bound by about 2 kcal/mol. This can be explained by the electrostatic potential of azulene, which only partially reflects the charge separation according to a $4n + 2$ π electron rule. The carbon atoms of the seven-membered ring define the region in the molecule with the least negative potential, and thus, these come closer together than, e.g., the five-membered rings. Furthermore, in the 7−7 arrangements, regions with positve potential at the hydrogens H4−H8 are quite close to C1/C3, where the potential is the most negative.

From the results of the EDA and the potential energy curves, we can conclude that energetically favored complexes of π stacked structures (i) have displaced or rotated arrangements that minimize exchange−repulsion but still allow good dispersion interactions, (ii) optimize electrostatic interactions by avoiding too-close contacts of regions with very negative electrostatic potential, and (iii) have significant orbital and charge-transfer contributions to binding that are, however, difficult to interpret with simple models.

The DFT-D approach has proven as a reliable and computationally fast tool to explore the conformational space of weakly bonded aromatic complexes. The success of this simple method for a complicated π system like azulene again demonstrates that the vdW interactions are quite unspecific and isotropic and that an accurate account of the first-order electronic effects (ES and POCT) is very important. However, the slight underbinding of DFT-D compared to SCS-MP2 for the azulene dimers results from the molecule-independent C_6 coefficients used that cannot account for the relatively large and specific polarizability of the monomer. Future work in this direction to further improve the ability of DFT for the important vdW interactions is currently in progress.

Acknowledgment. This work was supported by the Deutsche Forschungsgemeinschaft in the frameworks of the SFB 424 ("Molekulare Orientierung als Funktionskriterium in chemischen Systemen") and the international graduate college "template directed chemical synthesis". The authors thank C. Mück-Lichtenfeld for technical assistance.

(57) Robertson, J. M.; Shearer, H. M. M.; Sim, G. A.; Watson, D. G. *Acta Crystallogr.* **1962**, *15*, 1. Pawley, G. S. *Acta Crystallogr.* **1965**, *18*, 560. Bräuniger, T.; Pouoko, R.; Luz, Z.; Gutsche, P.; Meinel; Zimmermann, H.; Haeberlen, U. *J. Chem. Phys.* **2000**, *112*, 10858.

Supporting Information Available: Tables containing the DFT-D-BLYP/TZV2P optimized complex and monomer geometries (Cartesian coordinates) and corresponding DFT-D, MP2, and SCS-MP2 total energies. This material is available free of charge via the Internet at http://pubs.acs.org.

JA053613Q